Iranian Journal of Medical Physics
Vol. 13, No. 3, September 2016, 174-182
Received: July 22, 2016; Accepted: September 10, 2016

Original Article

Gamma Spectrometric Analysis of Iron Ore Samples of Arak, Iran

Reza Pourimani[1*], Hamid Reza Azimi[1]

Abstract

Introduction
Iron ore is one of the most important natural raw materials that is widely used for manufacturing iron and steel. This type of ore contains various amounts of radionuclides; thus, exposing workers handling their extraction, transportation, and processing to radiation.

Materials and Methods
In this study, 12 ore samples (each mass weighing about 2 kg) were collected from the iron ore mining areas of Arak region, Iran. The specific activities of ^{226}Ra, ^{232}Th, and ^{40}K were determined usinggamma-ray spectrometry method employing high-purity germanium (HPGe) detector.

Results
The specific activities of ^{226}Ra, ^{232}Th, and ^{40}K in samples were 9.39-271.70 Bq/kg, <1.68-60.98 Bq/kg, and 25.34-800.03Bq/kg, respectively. The doses received by workers handling these materials were estimated by using methods for dose assessment provided in a report by the European Commission. In transport, indoor storage, and outdoor storage scenarios, the effective doses due to the use Fe ore were 1.11-23.45 μSv/y, 1.69-39.22 μSv/y, and 1.46-33.78 μSv/y, respectively. For all the samples, the effective doses in different scenarios were lower than the intervention exemption level (1.0×10^{-3} Sv/y) suggested in International Commission of Radiological Protection (ICRP) Publication 82.

Conclusion
The gamma ray spectrometric analysis showed that the specific activities of natural radionuclides in samples, except for limonite ore, were within the worldwide range. The effective dose received by workers was much lower than the maximum acceptable value (1000 μSv/y); therefore, the level of radiations in this mine had no adverse consequences for public health.

Keywords: Dose assessment, Iron ore, Natural radiation, Radionuclide

1. Department of Physics, Faculty of Science, Arak University, Arak, Iran

*Corresponding author: Tel: 0918161224; Fax: +98 086-34173406; E-mail: r-pourimani@araku.ac.ir

1. Introduction

Assessment of natural radioactivity and the absorbed dose by the population is of paramount importance from people's health point of view. Natural radioactivity is present everywhere on earth in different levels depending on geographical situation and composition of rocks and soil. Humans are constantly exposed to radiation from decay of these radionuclides.

One of the main external sources of irradiation to human body is represented by gamma radiation terrestrial, emitted from the natural radioisotopes. Natural environmental radioactivity mainly arises from primordial radionuclides such as uranium (^{238}U), actinium (^{235}U), and thorium (^{232}Th) series and the radioactive isotopes of potassium (^{40}K) in soil, building materials, water, rocks, and atmosphere [1]. These radionuclides have been present in the environment since the formation of the earth.

The average of ^{238}U content in the Earth's crust has been estimated to be 2.7 mg/kg and its concentration may be as high as 120 mg/kg in phosphate rocks [2]. Meanwhile, the ^{232}Th average content of the Earth's crust is about 9.6 mg/kg [3]. Therefore, human beings and their environment are continuously exposed to these types of radiation, of which 81% can be attributed to natural radiation, with the remaining 19% coming from artificial sources [4]. Another natural source of radiation is cosmic ray originating from outer space [5]. A significant amount of artificial radionuclides (^{137}Cs and ^{90}Sr) is also present in soil, caused by testing of nuclear weapons in the atmosphere and nuclear accidents such as Chernobyl nuclear power plant in 1986 [6].

For the production of iron and steel many natural raw materials are necessary, the most important of which as to tonnage and value is iron ore. A material containing a significant amount of natural radioactive nuclides is referred to as a naturally occurring radioactive material (NORM). Workers who handle industrial materials containing NORMs at high concentrations are at risk of being exposed to radiation at considerable levels. The critical levels of NORMs necessitated further regulatory requirements provided in 2004 by the International Atomic Energy Agency (IAEA) Safety Guide [7]. The IAEA critical values are 1000 Bq/kg for ^{40}K and 100 Bq/kg for all other radionuclides with natural origin.

The present study was performed on iron ore samples collected from an ore mine in Arak, Iran. Mining operations in such Fe- and Mn-rich regions changes the level of natural radioactivity in the environment, which contributes to the collective radiation dose to the general population. These Fe and Mn mining activities have disturbed the ecology and environmental balance of the region [8,9]. Hence, we assessed the specific activities of radionuclides and radiological hazard due to gamma radiation in the environmental materials (ores) of the Fe ore.

This study can provide reference data on natural background radiation for this region, as there is a scarcity of studies in this area. The study also estimates the gamma dose rate (D) in air, annual gonadal equivalent dose (AGED), and excess lifetime cancer risk (ELCR) due to natural radioactivity for all samples, which can promote public awareness and provide information on radiological protection to the people. The total effective dose received by workers and drivers was calculated with assumption that they are exposing 1800 and 850 hours, respectively, and 200 hours for loading and unloading time for transportation scenario, for drivers which included inhalation and ingestion of dust.

2. Materials and Methods

2.1. Sample Collection and Preparation

The study region, a district about 56 km South-East of Arak lies at latitude of 33°47' N and longitude of 49°42' E, and its surrounding regions are rich sources of grade hematite, limonite, and goethite ore [10]. The topographic and geologic map of the study region is shown in Figure 1. This map was drawn by the authors according to topographic & geologic map of Shams Abad Mine prepared by Ramazany (the company supplies steel manganese of Iran).

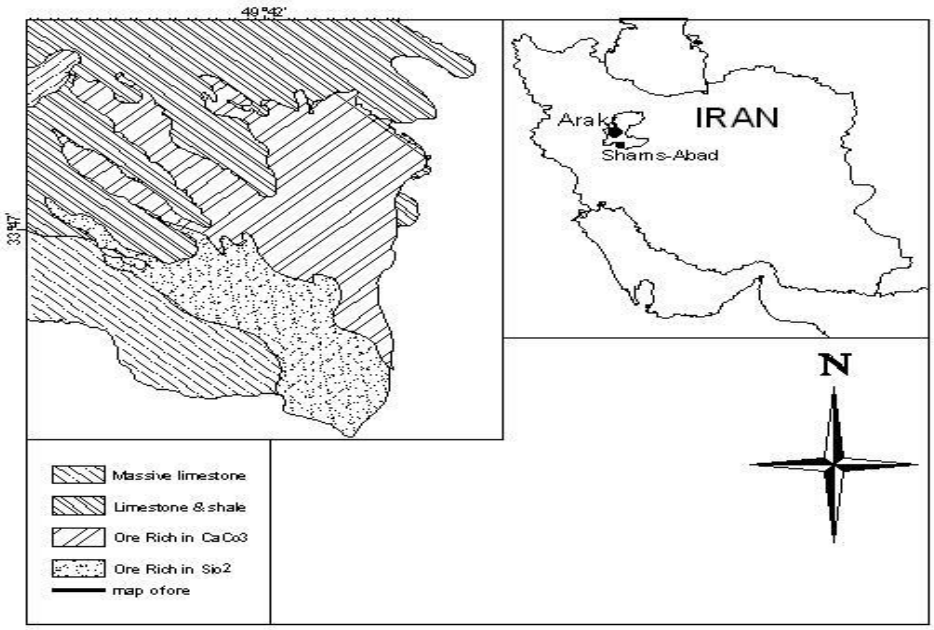

Figure 1. Topography and geological map of Shams-Abad mine

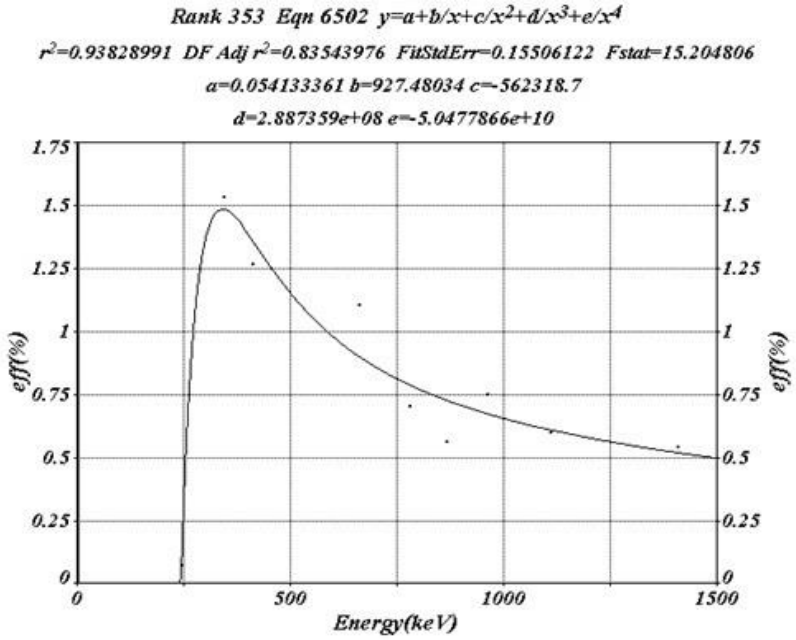

Figure 2. Calibration curve for HPGe GCD30195 detector

A total of 12 ore samples were collected from the iron ore mining areas of Arak region, with each mass weighing about 2 kg. The samples were collected from 20 different points and mixed according to color and kind of ore. The detailed information regarding the samples is provided in Table 1. All the samples were crushed, homogenized, and pulverized to a fine powder and sieved through a 50-mesh screen changing into fine powder in laboratory [11].

All the samples were placed in oven for drying at 100°C for 12 h to ensure that the moisture was completely removed. Samples were packed in Marinelli beaker container with 800 cc volume. Each sample was coded according to the ore composition. The mass of each sample were 950 g.

Table 1. Samples codes, main and sub components of iron ore samples

Sample No.	Sample code	Main components	Subcomponents
1	H	Hematite	
2	HGL1	Hematite	Goethite, Limonite
3	L1	Limonite	
4	L2	Limonite	
5	HGM	Hematite	Goethite, Malachite
6	HGL2	Hematite	Goethite, Limonite
7	GHL	Goethite	Hematite, Limonite
8	GB	Goethite	Barite
9	HGLSi1	Hematite	Goethite, Limonite, Silicon
10	HGS	Hematite	Goethite, Siderite
11	HGGa	Hematite	Goethite, Galen
12	HGLSi2	Hematite	Goethite, Limonite, Silicon

The collected samples required particular care since radon is a short-lived gaseous nuclide and tends to escape from the samples. In this work, standard containers were sealed. After the minimum 50 days of preparing sealed samples, gamma ray spectra were registered. This time is necessary for taking radioactive chain equilibrium, where the decay rate of the daughters became equal to that of the parents [12].

2.2. Gamma Ray Spectrometry

Specific activity measurements were performed by gamma ray spectrometry method employing high purity germanium (HPGe) P-type coaxial detector (GCD30195BSI) manufactured by Baltic Scientific Instrument LTD (005-Latvia) with 30% relative efficiency, which is connected to a multi-channel analyzer of 8192 channels, was employed. The energy resolution (full width at half maximum) of this detector is 1.95 keV for gamma energy line at 1332.520 keV due to ^{60}Co and a Peak-to-Compton ratio of 60; operating voltage was 3000 V.

The detector and preamplifier are shielded in a chamber of three layers composed of 10 cm thick lead, 1.5 mm thick cadmium, and 3 mm thick by copper. This shield serves to reduce background radiation. The soft components of cosmic ray, consisting of photons and electrons, are reduced to a very low level by 100 mm of lead shielding. The X-ray (73.9 keV) emitted from lead by its interaction with external radiation is suppressed by copper layer and cadmium layer successively, absorbing thermal neutrons produced by cosmic ray [13].

Table 2. Dose conversion factor, dilution factor, breathing rate, dust concentration and ingestion rate in each scenario.

	Transport scenario			Indoor storage scenario			Outdoor storage scenario		
	External	Inhalation	Ingestion	External	Inhalation	Ingestion	External	Inhalation	Ingestion
T_e(y^{-1})	850	100	100	1800	1800	1800	1800	1800	1800
F_d	1	1	1	1	1	1	1	1	1
B_r (m^3 /h)	1.2	1.2	1.2	1.2	1.2	1.2	1.2	1.2	1.2
C_{dust} (g /m^3)	0.001	0.001	0.001	0.0005	0.0005	0.0005	0.0002	0.0002	0.0002
R_{ing} (g/h)	0.01	0.01	0.01	0.01	0.01	0.01	0.01	0.01	0.01
D_{ext}(μSv/h Bq/g), D_{inh}(μSv/g) and D_{ing}(μSv/g) for ^{238}U	0.077	29	2.6	0.032	29	2.6	0.032	29	2.6
D_{ext}, D_{inh} and D_{ing} for ^{232}Th	0.12	48	1.1	0.047	48	1.1	0.048	48	1.1
D_{ext}, D_{inh} and D_{ing} for ^{40}K	0.0076	0	0	0.0029	0	0	0.0029	0	0

To minimize the effect of scattering radiation from the shield, the detector was located in the center of the chamber. The samples were placed in the face to face geometry over the detector. Finally, the spectra were registered using the Lsrmbsi software. The relevant efficiency calibration with consideration of coincidence correction transition was carried out for Marinelli Beaker standard source including ^{241}Am, ^{152}Eu, and ^{137}Cs, covering an energy range of 59.5-2000 keV. According to the registered gamma ray spectrum, the absolute efficiency of the detector configuration was calculated as [11]:

$$\varepsilon = \frac{\mathrm{N_i}}{\mathrm{Act}\times \mathrm{P_n(E_i)}\times \mathrm{T}} \times 100 \qquad (1)$$

Where *Act* is activity concentration in Bq, N_i is the net count under the full-energy peak corresponding to the E_i energy, $P_n(E_i)$ is the photon emission probability for the particular energy E_i, and *t* is the counting time. The efficiency (%) for each gamma energy E_i (keV) was calculated with table curve software and fitted to experimental data by polynomial curve

$$y = a + \frac{b}{x} + \frac{c}{x^2} + \frac{d}{x^3} + \frac{e}{x^4} \qquad (2)$$

where *y* is efficiency, *x* is gamma energy in keV, *a*, *b*, *c*, *d*, and *e* are fitted coefficients whose values are *a=0.054133361*, *b=927.48034*, *c=-562318.7*, *d=2.887359e+08*, and *e=-5.0477866e+10* (Figure 2). Using the above function the efficiency for different energies can be calculated.

2.3. Activity Measurement

Gamma ray spectrum of each sample was registered for 86400s (24 h). Assuming the daughter products of Ra and Th were in equilibrium, the ^{226}Ra activity of samples was estimated from the gamma emissions of ^{214}Pb (351.93keV) and ^{214}Bi (609.31keV). The gamma ray energies from ^{212}Pb (238.6 keV), ^{228}Ac (911.21, 968.97 keV), and ^{208}Tl (583.2 keV) were used to determine the specific activity of ^{232}Th. The activity concentration of ^{40}K was measured directly using its own gamma ray (1460.75 keV). Registered gamma ray spectra were analyzed and specific activities were calculated using Gamma vision32 EG & Ortec software. In all the analyzed spectra, correction was performed for background gamma ray spectra measured for empty Marinelli container in the similar condition.

Activity concentrations were calculated using the intensity of several γ-rays emitted by a nuclide as [11]:

$$Act(Bq/kg) = \frac{Net\ Area}{\varepsilon \times BR(\%) \times t \times m} \times 100 \qquad (3)$$

where *Net Area* is the net count under peak, *Act* (Bq/kg) is the specific activity, ε is the energy efficiency for gamma ray by detector, *BR* is the branching ratio of gamma ray intensity (%), *t* is the time of spectra in sec, and *m* is the mass of samples in kg.

2.4. Dose Assessment

Dose assessments for workers handling the ores during the exploitation and transportation of materials (transport scenario), the indoor storage of moderate amounts in warehouse (indoor storage scenario), and the outdoor storage of materials in large amount (outdoor storage scenario) were carried out by using the following methods, which were based on the recommended methods described in the Radiation Protection 122 (RP 122) publications of the European Commission [14]. The effective dose of external gamma radiation, inhalation, and ingestion exposure in each exposure pathway was calculated as [15]:

$$E_{ext} = D_{ext} \times T_e \times F_d \times A \qquad (4)$$

$$E_{inh} = D_{inh} \times T_e \times F_d \times B_r \times C_{dust} \times A \qquad (5)$$

$$E_{ing} = D_{ing} \times T_e \times F_d \times R_{ing} \times A \qquad (6)$$

where E_{ext}, E_{inh}, and E_{ing} are the effective doses due to external gamma radiation, inhalation, and ingestion exposures in Sv/y. D_{ext}, D_{inh}, and D_{ing} are the dose coefficients for external gamma radiation, inhalation, and ingestion exposures in Sv/h, Sv/g, and Sv/g, respectively. T_e is the exposure time (y^{-1}), F_d is the dilution factor, A is the specific activities of radionuclides in samples (Bq/g), B_r is the breathing rate (m^3/h), C_{dust} is the dust concentration during exposure time (g/m^3), and R_{ing} is the ingestion rate (g/h) [15]. The factors used for estimation of total effective dose received by workers are exhibited in Table 2. Natural resources such as ores mainly

contain ^{238}U series, ^{232}Th series, and ^{40}K. Therefore, the following equations were used to estimate the total effective dose received by each worker.

$$E_{ext(total)} = E_{ext(U)} + E_{ext(Th)} + E_{ext(K)} \quad (7)$$

$$E_{inh(total)} = E_{inh(U)} + E_{inh(Th)} + E_{inh(K)} \quad (8)$$

$$E_{ing(total)} = E_{ing(U)} + E_{ing(Th)} + E_{ing(K)} \quad (9)$$

$$E_{total} = E_{ext(total)} + E_{inh(total)} + E_{ing(total)} \quad (10)$$

where $E_{ext(U)}$, $E_{ext(Th)}$, and $E_{ext(K)}$ are the external effective doses induced by ^{238}U, ^{232}Th series, and ^{40}K, respectively, in Sv/y. $E_{inh(U)}$, $E_{inh(Th)}$, and $E_{inh(K)}$ are the inhalation effective doses and $E_{ing(u)}$, $E_{ing(Th)}$, and $E_{ing(K)}$ are the ingestion effective dose for corresponding radionuclides, respectively, in Sv/y. E_{total} is the sum of theses doses, which can be received by workers [15].

2.5. Annual Gonadal Dose Equivalent (AGDE)

The organs of interest by UNSCEAR include the thyroid, the lungs, bone marrow, bone surface cell, the gonads, and the female breast [16]. Therefore, the AGDE due to the specific activities of ^{226}Ra, ^{232}Th, and ^{40}K in soil and rock was calculated as [16]:

$$AGDE(\mu Sv/y) = 3.09\, A_{Ra} + 4.18 A_{Th} + 0.314 A_K \quad (11)$$

Where A_{Ra}, A_{Th}, and A_K are the average activity concentrations (Bq/kg) of ^{226}Ra, ^{232}Th, and ^{40}K, respectively.

2.6. Excess lifetime cancer risk (ELCR)

Excess lifetime cancer risk (ELCR) is calculated as [17]:

$$ELCR = AEDE \times DL \times RF \quad (12)$$

Where AEDE, DL, and RF are the annual effective dose equivalent, duration of life (70 years), and risk factor (0.05 Sv^{-1}), respectively. AEDE is calculated as [18]:

$$\text{AEDE Outdoor } (\mu Sv/y) = D(nGy/h) \times 8760(h/y) \times 0.7 \times 0.2 \times 10^{-3} \quad (13)$$

The value of D is dose rate in air at one meter height from ground that is calculated as [18]:

$$D\left(\frac{\mu Gy}{h}\right) = (0.462 A_{Ra} + 0.604 A_{Th} + 0.0417 A_K) \times 10^{-3} \quad (14)$$

where A_{Ra}, A_{Th}, and A_K are the average activity concentrations ($Bqkg^{-1}$) of ^{226}Ra, ^{232}Th, and ^{40}K, respectively.

3. Results

In this study, we determined the specific activities of ^{226}Ra, ^{232}Th, and ^{40}K in 12 samples of iron ore. Results of these measurements are shown in Table 3, and results of calculation of absorbed dose rate in air in one meter height from surface above the soil and rock (D), annual effective dose rate outdoor ($AED_{outdoor}$), annual gonadal equivalent dose (AGED), and excess lifetime cancer risk (ELCR) were calculated and shown in Table 4. The total effective dose received by workers who handle extraction of the raw mine materials and transportation of these materials to factories in different scenarios were calculated and demonstrated in Table 5.

Table3. The activity concentrations of ^{226}Ra, ^{232}Th and ^{40}K determined in iron ore samples of Arak zone

Sample no.	Sample code	^{226}Ra (Bq/kg)	^{232}Th (Bq/kg)	^{40}K (Bq/kg)
1	H	24.34±0.51	6.16±0.52	67.85±1.76
2	HGL1	36.92±0.61	13.21±1.03	134.37±2.73
3	L1	96.92±0.97	60.98±1.22	800.03±6.47
4	L2	271.70±1.84	11.58±1.68	102.96±6.38
5	HGM	57.23±0.74	8.64±0.75	186.93±3.92
6	HGL2	25.53±0.54	13.28±0.85	199.63±3.30
7	GHL	91.64±1.13	27.86±1.44	383.82±4.78
8	GB	9.39±0.53	<1.68	29.02±1.84
9	HGLSi1	42.30±0.74	4.68±0.73	87.26±3.03
10	HGS	76.39±0.86	22.16±1.39	509.13±5.55
11	HGGa	16.27±0.43	7.48±0.87	25.34±2.14
12	HGLSi2	19.87±0.47	5.48±0.71	87.52±2.70
Mean		64.04	15.27	217.82

Table 4. The mean gamma ray absorbed dose rate and dose related parameters for the iron ore samples and transport scenario

Sample code	D (nGy/h)	AED outdoor (μSv/y	AGDE (μSv/y	ELCR (10^{-4})	Transport scenario (μSv/y)			
					$E_{ext(total)}$	$E_{inh(total)}$	$E_{ing(total)}$	E_{total}
H	17.80±0.40	21.83	122.26	0.8	2.85	0.12	0.07	3.04
HGL1	30.64±0.69	37.58	211.49	1.3	4.92	0.20	0.11	5.23
L1	114.97±0.90	141.00	805.59	4.9	18.48	0.69	0.32	19.48
L2	136.81±1.35	167.78	920.29	5.9	21.72	1.01	0.72	23.45
HGM	39.45±0.59	48.38	271.65	1.7	6.27	0.25	0.16	6.68
HGL2	28.14±0.59	34.51	179.08	1.2	4.51	0.16	0.08	4.76
GHL	75.17±1.03	92.19	520.14	3.2	12.02	0.48	0.27	12.77
GB	6.56±0.26	8.05	45.15	0.3	1.04	0.04	0.02	1.11
HGLSi1	26.01±0.57	31.90	177.67	1.1	4.13	0.17	0.11	4.42
HGS	69.91±0.96	85.74	488.54	3.0	11.14	0.39	0.22	11.75
HGGa	13.09±0.57	16.05	89.50	0.6	2.12	0.10	0.05	2.26
HGLSi2	16.14±0.49	19.79	111.79	0.7	2.58	0.10	0.06	2.74
Mean	47.89	58.73	330.10	2.06	7.64	0.31	0.18	8.14

Table 5. Calculated the effective dose received by workers in each scenario

Sample code	Indoor storage scenario (μSv/y)				Outdoor storage scenario (μSv/y)			
	$E_{ext(total)}$	$E_{inh(total)}$	$E_{ing(total)}$	E_{total}	$E_{ext(total)}$	$E_{inh(total)}$	$E_{ing(total)}$	E_{total}
H	2.28	1.08	1.26	4.62	2.29	0.43	1.26	3.98
HGL1	3.94	1.84	1.99	7.78	3.97	0.73	1.99	6.69
L1	14.92	6.20	5.74	26.86	15.03	2.48	5.74	23.25
L2	17.16	9.11	12.94	39.22	17.19	3.64	12.94	33.78
HGM	5.00	2.24	2.85	10.09	5.02	0.89	2.85	8.76
HGL2	3.64	1.49	1.46	6.58	3.66	0.59	1.46	5.71
GHL	9.64	4.31	4.84	18.79	9.69	1.73	4.84	16.25
GB	0.83	0.38	0.47	1.69	0.84	0.15	0.47	1.46
HGLSi1	3.29	1.57	2.07	6.93	3.29	0.63	2.07	5.99
HGS	8.93	3.54	4.01	16.49	8.97	1.42	4.01	14.40
HGGa	1.70	0.89	0.91	3.51	1.72	0.36	0.91	2.98
HGLSi2	2.06	0.90	1.04	4.01	2.07	0.36	1.04	3.47
Mean	6.11	2.80	3.30	12.21	6.14	1.12	3.30	10.56

4. Discussion

The specific activity of ^{226}Ra in samples varied from 9.39 Bq/kg to 96.92 Bq/kg, with an average of 64.04 Bq/kg, which is greater than the global average of 32 Bq/kg. For ^{232}Th and ^{40}K, this value varied from MDA to 60.98 Bq/kg with an average of 15.27 Bq/kg and from 25.34 Bq/kg to 800.03 Bq/kg with an average of 217.82 Bq/kg, respectively, which were less than the global averages of 45 Bq/kg and 412 Bq/kg, respectively. The minimum detectable activity of the radionuclide ^{232}Th is 1.68 Bq/kg. The value of specific activities of the corresponding radionuclides in hematite, goethite, and siderite ore samples from the Arak mines were within the range of worldwide values [19].

The absorbed dose rates due to gamma radiation was found to be in the range of 6.56-136.81 nGy/h with a mean of 47.89 nGy/h for the ore samples, which is less than the global average of 55 nGy/h [19]. The mean value of annual effective dose outdoor was 58.73 μSv/y.

Radiation in the alteration regions was more than the rocky intact regions. During the performance of underground water, accumulation of radionuclides was observed in alteration regions or limonite ores [20]. The alteration phenomenon (conversion of hematite ore to limonite ore) with headway flows, cause washing and exiting radionuclides and other metallics or nonmetallics from host rocks and put the radionuclides in a stable chemical field. In addition, in the alteration phenomenon, pH and Eh roles are very important. In the acidic pH, radionuclides are solution and in the pH greater than 5, radionuclides absorb Fe hydroxide (limonite), aluminum, and manganese. This situation is optimal in alkaline conditions [21]. In other words, there is an inverse relationship between pH and the activity concentration. Thus, in high pH under reducing conditions in alkaline environments, activity concentration is low and conversely, the absorption of radionuclides by limonite ores, manganese, and aluminum is more in the alkaline conditions.

AEDE and AGDE values are listed in Table 4. The values of AGDE varied from 45.15 to 920.29μSv/y, and the average value was found to be 330.10μSv/y. The average values of AGDE were found to be 550.50 and 2398 μSv/y for Rize in Turkey and Eastern Desert of Egypt, respectively [22, 23]. These values of AGDE were higher than our obtained results.

The calculated range of ELCR is 0.326×10^{-3}-1.067×10^{-3}, with an average of 0.700×10^{-3} for the samples. This average value of ELCR is twice the global average (0.290×10^{-3}), but is less than the maximum acceptable value (10^{-3}) [19]. The effective dose received by workers for transportation scenario varied from 1.11 μSv/y to 23.45 μSv/y with mean value of 8.14 in μSv/y and for indoor storage and outdoor storage scenarios varied from 1.69 μSv/y to 39.22 μSv/y and 1.46 to 33.78 μSv/y with mean values 12.21 μSv/y and 1.56 μSv/y, which was lower than the intervention exemption levels (1.0×10^{-3} Sv/y) proposed in International Commission of Radiological Protection (ICRP) Publication 82 [24].

5. Conclusion

The ore samples collected from Arak were studied for the concentrations of the three primordial radionuclides using gamma ray spectrometry method. The results of this study evaluated specific activates of radionuclides increase in ores containing limonite mineral composition. The average value of ELCR was more than twice the global average (0.290×10^{-3}), but was less than the maximum acceptable value of 10^{-3}. The annual effective dose received by workers handling transportation and indoor and outdoor storage scenarios was lower than the intervention exemption level of 1000 μSv/y. Therefore, the level of radiations in this region had no consequences for public health. The results of this work can be used as reference data for future measurements.

Acknowledgements

The authors would like to thank Arak University Research Council for their financial support.

References

1. UNSCEAR (United Nations Scientific Committee on the Effects of Atomic Radiation). Sources and effects of ionizing radiation report to general assembly with scientific Annexes. New York, United Nation Publication, 1993.
2. Singh P, Rana N, Naqavi A and Rivastava D. Levels of uranium in water from some Indian cities determined by Fission Track Analysis. Radiation Measurements. 1996; 26(5):683-7. DOI:10.1016/S1350-4487(97)82882-X.
3. Firestone RB, Shirley VS, Baglin CM. Table of isotopes CD-ROM. Eight Edition Version. 1996 Mar.1.

4. De Castro LP, Maihara VA, Silva PSC, Figueira RCL. Artificial and natural radioactivity in edible mushrooms from Sao Paulo, Brazil. Journal of Environmental Radioactivity. 2012; 113:150-4. DOI: 10.1016/j.jenvrad.2012.05.028.
5. El-Arabi AM. 226Ra, 232Th and 40K concentrations in igneous rocks from eastern desert, Egypt and its radiological implications. Radiation Measurements. 2007; 42(1):94-100. DOI: 10.1016/j.radmeas.2006.06.008.
6. Kannan V, Rajan MP, Iyengar MAR, Ramesh. R. Distribution of natural and anthropogenic radionuclides in soil and beach sand samples of Kalpakkam (India) using hyper pure germanium (HPGe) gamma ray spectrometry. Applied Radiation and Isotopes. 2002; 57(1):109-19. DOI:10.1016/S0969-8043(01)00262-7.
7. IAEA, 2004. International Atomic Energy Agency, Application of the Concepts of Exclusion, Exemption and Clearance, Safety Standards Series No. RS-G-1.7. IAEA,Vienna.
8. Abdel-Ghany HA. Natural Activities of 238U, 232Th and 40K in Manganese ore. American Journal of Environmental Sciences, 2010; 6(1): 90-4. DOI : 10.3844/ajessp.2010.90.94.
9. Ebaid YY, El-Tahawy MS, El-Lakany AA, Garcia SR, Brooks GH. Environmental Radioactivity Measurements of Egyption Soils. Journal of Radioanalytical and Nuclear Chemistry. 2000; 243(2):543-50. DOI: 10.1023/A:1016075508765.
10. Farhadi R. The study of geological, geochemical analysis, facies and genesis of deposits of iron, manganese in Shams-Abad of Arak. MS thesis, Faculty of Science, Tarbiat Modaress University, Tehran, Iran. 1996.
11. IAEA-TECDOC-1360. Collection and preparation of bottom sediment samples for analysis of radionuclides and trace elements. International Atomic Energy Agency.2003.
12. L'Annonziata M. Handbook of Radioactivity analysis. Third Edition Academic Press access online by Elsevier Amazoon.com, 2012.
13. Aziz A. Methods of Low-Level Counting and Spectrometry Symposium. Berlin. 1981; 221.
14. EC. European Commission, Practical Use of the Concepts of Clearance and Exemption (Part II). EC, 2002, Belgium.
15. Kazuki Iwaoka, Keiko Tagami, Hidenori Yonehara. Measurement of natural radioactive nuclide concentrations in various metal ores used as industrial raw materials in Japan and estimation of dose received by workers handling them. Journal of Environmental Radioactivity. 2009; 100: 993–7. DOI: 10.1016/j.jenvrad.2009.08.004.
16. UNSCEAR (2010). Sources and Effects of Ionizing Radiation. Report to the General Assembly, with scientific annexes. 1:1-219.
17. ICRP (International Commission on Radiological Protection), Recommendations of the International Commission on Radiological Protection, Publication 60. 1990, Vol. 21, No.1 – 3, .
18. Beretka J, Mathew PJ. Natural radioactivity of Australian building materials, industrial wastes and by products. Health Phys. 1985; 48: 87-95.
19. UNSCEAR (United Nations Scientific Committee on the Effects of Atomic Radiation). Sources and effects of ionizing radiation report to general assembly with scientific Annexes. New York, United Nation Publication, 2008.
20. Pirlo MC, Giblin AM. Application of groundwater–mineral equilibrium calculations to geochemical exploration for sediment-hosted uranium observations from the Frome Embayment, South Australia. Geochemistry Exploration Environment Analysis. 2004; 4(2):113–27. DOI: 10.1144/1467-7873/03-027.
21. Doulati Ardejanii F, Rooki R, Jodieri Shokri B, Eslam Kish T, Aryafar A, Tourani P. Prediction of Rare Earth Elements in Neural Alkaline Mine Drainage from Razi Coal Mine, Golestan Province, Northeast Iran, Using General Regression Neural Network. Journal of Environmental Engineering. 2013; 139(6):896-907. DOI: 10.1061/(ASCE)EE.1943-7870.0000689.
22. Kurnaz A, Kucukomeroglu B, Keser R, Okumusoglu NT, Korkmaz F, Karahan G, Cevik U. Determination of radioactivity levels and hazards of soil and sediment samples in Firtina Valley (Rize, Turkey). Applied Radiation and Isotopes. 2007; 65(11): 1281-89. DOI: 10.1016/j.apradiso.2007.06.001.
23. Arafa W. Specific activity and hazards of granite samples collected from the Eastern Desert of Egypt. Journal of Environmental Radioactivity. 2004; 75(3):315–27. DOI: 10.1016/j.jenvrad.2004.01.004.
24. ICRP. Protection of the Public in Situations of Prolonged Radiation Exposure ICRP Publication 82, 1999.